Crossover from chaotic to self-organized critical dynamics in jerky flow of single crystals

G. Ananthakrishna,[1,2,*] S. J. Noronha,[1] C. Fressengeas,[3] and L. P. Kubin[4]
[1]*Materials Research Centre, Indian Institute of Science, Bangalore 560 012, India*
[2]*Center for Condensed Matter Theory, Indian Institute of Science, Bangalore 560 012, India*
[3]*Laboratoire de Physique et Mécanique des Matériaux, CNRS UMR No. 7554, Université de Metz, Ile du Saulcy, 57045 Metz Cedex 01, France*
[4]*Laboratoire d'Etude des Microstructures, CNRS-ONERA (OM), 29, Avenue de la Division Leclerc, Boîte Postale 72, 92232 Chatillon Cedex, France*
(Received 17 May 1999)

We report a crossover from chaotic to self-organized critical dynamics in the Portevin–Le Chatelier effect in single crystals of Cu–10% Al in tension as a function of the applied strain rate. For low and intermediate strain rates, we provide an unambiguous support for the existence of chaotic stress drops by showing the existence of a finite correlation dimension and a stable positive Lyapunov exponent. A surrogate data analysis rules out the possibility that the time series is due to a power law stochastic process. As the strain rate is increased, the distributions of stress drops and the time intervals between the stress drops change from peaked to power law type with an exponent close to unity reminiscent of self-organized critical state. A scaling relation compatible with self-organized criticality relates the various exponents. The absence of a finite correlation dimension and a stable positive Lyapunov exponent at the highest strain rate also supports the evidence of crossover. [S1063-651X(99)11011-0]

PACS number(s): 05.45.−a, 62.20.Mk

I. INTRODUCTION

Repeated stress drops followed by periods of reloading are observed in many interstitial and substitutional metallic alloys when tensile specimens are deformed in a certain range of strain rates and temperature [1,2]. This phenomenon is referred to as the Portevin–Le Chatelier (PLC) effect or jerky flow. It is one of the best studied forms of plastic instability due, in particular, to the interest in removing the loss of ductility and surface roughness associated with the phenomenon. The physical origin of the effect is the dynamic interaction of two defect populations, namely, mobile dislocations and solute atoms. Mobile dislocations which are carriers of plastic strain rate move jerkily between the obstacles provided by other dislocations. Solute atoms diffuse in the stress field generated by mobile dislocations, and further pin them while they are arrested at obstacles. When the system is in a certain range of strain rates and temperatures, the diffusion time of the solute atoms is of the order of the waiting time of dislocations at obstacles, a force versus negative dislocation velocity relationship may occur which at the specimen's scale translates to negative strain rate sensitivity of the flow stress [2–6]. As a consequence, the classical picture of the PLC effect is that of an instability of the uniform state of tensile deformation due to the anomalous negative strain rate sensitivity [5]. The instability manifests itself by nucleation of bands of localized plastic deformation with a typical width of 10–100 μm, each band being associated with a stress drop on the stress versus time curve. Depending on the temperature and strain rate conditions, these bands may or may not propagate along the sample [3]. Different possibilities of correlation in space (or the lack of it) of the bands also exist. Thus a rich variety of spatiotemporal behavior is displayed. The objective of the present paper is to analyze the structure of the serrated stress versus time series in single crystal samples when the applied strain rate is varied.

The influence of concepts and methods of dynamical systems on the studies of the PLC effect has been considerable. In the last few years, starting from a dynamical description, attempts have been made to recover the complex spatiotemporal patterns emerging from this instability (see, e.g., the collection of papers in Ref. [3]). Our interest in the dynamical analysis of the serrations was triggered off by a prediction of chaotic stress drops based on a model due to Ananthakrishna and co-workers [6]. These authors used a coupled set of equations for the evolution of three dislocation populations, one of which interacts with solute atoms. These equations are dynamically coupled to the ''machine equation'' which determines the stress rate in the sample as a result of constant applied strain rate and the resultant plastic strain rate. Apart from predicting several general features of the PLC effect including the most dominant feature, namely, the negative strain rate sensitivity of the flow stress, the model also predicts that chaotic behavior should be observed within a certain range of applied strain rates [7,8]. The possibility of chaos was also suggested later by Jeanclaude *et al.* [9] in the framework of a spatiotemporal model for the PLC band propagation.

In order to verify this prediction, several experiments have been carried out aimed at characterizing the structure of the recorded stress-time series. The first attempt in this direction was performed on single crystals of Cu-Al alloys [10] using the method of Grassberger and Procaccia [11] to estimate the correlation dimension. This preliminary analysis

*Also at Jawaharlal Nehru Centre for Advanced Scientific Research, Bangalore 560 064, India. Electronic address: garani@mrc.iisc.ernet.in

and further results using complementary methods including the singular value decomposition and the positive Lyapunov exponent determination provided substantial evidence of chaotic behavior [12], but on short data sets ($\sim$6000 points), often with high levels of noise. For this reason, specific experiments were performed on Al-Mg polycrystals in order to obtain reasonably long, accurate, and nearly noise-free stress signals. The analysis of these data using the correlation dimension, the singular value decomposition, the Lyapunov exponents and surrogate analysis showed unambiguously that they are of deterministic chaotic origin [13]. There is also a report from another group [14] who calculated only the positive exponent on a very short time series ($\sim$2500 points), which renders the results of the analysis less reliable.

A different approach to the study of the PLC stress drops was recently undertaken [15,16] through a statistical analysis. This study showed that statistics of stress drops can exhibit either a peaked or a power law distribution depending on experimental conditions such as the applied strain rate and the temperature, thus suggesting various dynamical regimes. The power law distribution is reminiscent of self-organized critical (SOC) state where events of all magnitudes occur [17], whereas a peaked distribution is observed to be associated with chaos in the analysis of our experimental signals. The existence of a chaotic dynamics in the PLC instability under one strain rate condition does not preclude the possibility of a SOC-type dynamics under a different strain rate condition. This, in fact, is a distinct possibility, since it is a spatially extended driven system with a built-in threshold for the onset of stress drops [3,6]. Since our results on chaotic stress drops were obtained at low and intermediate strain rates, and power law distributions have been reported at high strain rates [15,16], in this paper we investigate the possibility of a crossover in the dynamics as the strain rate is increased. Toward this aim, we use well known quantifiers of deterministic chaotic signals, namely, the correlation dimension [11], the Lyapunov spectrum [18–20], and a surrogate data analysis of each of the time series as indicators of the changes as the crossover occurs. Further, the distributions of the stress drop magnitudes and intervals are also studied for a statistical characterization. This analysis is carried out on single crystal specimens in order to take advantage of the wide range of strain rates that was available.

The outline of the paper is as follows. Section II contains experimental details. In Sec. III, we briefly outline the methods used for time series analysis. We present the results in Sec. IV. Finally, Sec. V is devoted to discussion and conclusions.

II. EXPERIMENTS

Specimens of metallic alloys in the form of thin plates are loaded in a tensile testing machine at a constant crosshead velocity, thus providing a quasiconstant average strain rate $\dot{\epsilon}_a$. The total extension of the system is the sum of elastic and plastic parts. The elastic part itself has contributions arising from the extension of the sample and the machine. The so-called machine equation can therefore be written as

$$\dot{\sigma} = M\left[\dot{\epsilon}_a - \frac{1}{L}\int_0^L \epsilon_p(x,t)\,dx\right], \tag{1}$$

where M is the combined elastic constant of the specimen and the machine, and L is the length of the sample. We have neglected inertial effects since stress equilibrates at the velocity of sound on a much shorter time scale than any other intrinsic time scale. Thus the axial stress σ is constant over the entire sample, although it generally results from the contributions of many events of localized plastic deformation occurring in different parts of the specimen. In experiments, the stress signal σ is monitored by a load cell located at one end of the sample.

The experiments on Cu–10% Al single crystals were performed at Braunschweig Technical University. In general, the range of strain rates where the PLC effect is seen depends on temperature apart from other material parameters such as the alloy composition and microstructure. In the case of Cu–10%Al, the boundary for the onset of the PLC effect in the strain rate and temperature variables is itself complex [21]. Thus there is no identifiable time scale with respect to which the applied strain rate can be represented in a scaled form. One point of relevance here is the fact that the PLC effect is seen at relatively high temperature compared to other room temperature alloys like Al-Mg. The samples were initially homogenized for 36 h at 1230 K. Then single crystal samples oriented for easy glide were deformed at a temperature of 620 K. In the domain of occurrence of the PLC effect, three files containing 4×10^4, 2×10^4, and 1.2×10^4 points were recorded at strain rates 3.3×10^{-6} 5^{-1}, 1.7×10^{-5} 5^{-1}, and 8.3×10^{-5} 5^{-1}, respectively (roughly separated by a factor of 5). The sampling rate was 20 Hz. We shall refer to these files as PLC files *l*, *m*, and *h*, respectively.

In general, in tensile loading of metallic alloys, there is an upward drift of the stress-time curve, usually referred to as strain hardening. This effect originates from the accumulation of dislocations in the sample. The low and intermediate strain rate curves showed very little strain hardening. However, the highest strain rate data showed low but noticeable strain harding which was removed in our analyses by subtracting a moving average. Plots of the PLC files *l*, *m*, and *h* for a short duration of time are shown in Figs. 1(a)–1(c) to give an idea of the structure of the stress drops. As can be seen, at the lowest strain rate (PLC file *l*), we have large stress drops with very few small ones. In contrast, the highest strain rate case (PLC file *h*) has numerous small drops and fewer large ones. As will be discussed below, this well known feature of the PLC effect is due to shortening of the time scale of dislocation mobility as the applied strain rate is increased.

III. METHODS OF ANALYSIS

We follow conventional methods for the analysis of the time series by calculating the correlation dimension and the Lyapunov spectrum. Both methods start with the phase space reconstruction of the attractor by embedding the time series in a higher dimensional space using the time delay technique [22].

Consider the stress signal defined by

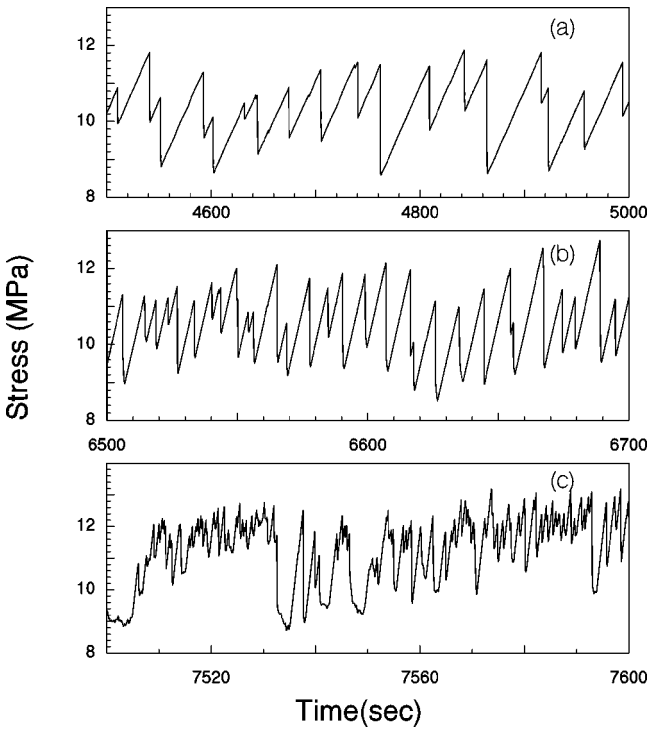

FIG. 1. (a)–(c) Time series data for the PLC *l*, *m*, and *h* files showing the fine structure of the time series.

$$[\sigma(k), k=1,2,\ldots,N], \tag{2}$$

where the index k is in units of the time increment Δt. Let

$$\vec{\xi}_k=[\sigma(k),\sigma(k+\tau),\ldots,\sigma(k+(d-1)\tau)],$$
$$k=1,\ldots,[N-(d-1)\tau] \tag{3}$$

be a vector defined by embedding the signal with a time delay τ in a d-dimensional space. Once the reconstructed attractor is obtained, its self-similar nature is quantified by calculating appropriate dimensional quantities. The simplest is the correlation dimension which is obtained by using a popular algorithm due to Grassberger and Procaccia [11]. The correlation integral is defined as the fraction of the pairs of points $\vec{\xi}_i$ and $\vec{\xi}_j$ whose distance is less than a specified value r,

$$C(r)=\frac{1}{N_p}\sum_{i,j} H(r-|\vec{\xi}_i-\vec{\xi}_j|), \tag{4}$$

where $H(\cdot)$ is the Heaviside function and N_p is the number of pairs used in the sum. The self-similar structure is reflected in the scaling relation $C(r)\sim r^{\nu}$ in the limit of small r, where ν is the correlation dimension. As the embedding dimension d is increased, the slope $\ln C(r)/\ln r$ tends to a constant value ν, taken as the correlation dimension. In practice, due to limited length of the time series and noise superimposed on the signal, one looks for a scaling regime at intermediate length scales of r, for some values of embedding dimension. However, the existence of a finite correlation dimension is not by itself a compelling reason for the time series to be of chaotic origin, since it can also arise due to a power law stochastic process [23–25]. However, it has been pointed out that it is possible to use the existence of a finite correlation dimension as a method of discriminating a dynamical time series as against a stochastic one [24] by introducing the method of surrogate data analysis. Surrogate data sets for each time series are obtained by randomizing the phases of the signal's Fourier transform, and Fourier inverting them. Eighteen to twenty four surrogate data sets have been generated for all our original files. For each of these surrogate data sets, the slopes of $\ln C(r)/\ln r$ for various d values are calculated. If the slopes increase with the embedding dimension d, in contrast with the original file for which it saturates, it can be concluded that the latter is of deterministic origin.

Since Lyapunov exponents are considered as unambiguous quantifiers of chaotic dynamics, we have also analyzed the time series for the existence of a stable positive and zero Lyapunov exponent. Conventional algorithms for calculating the Lyapunov spectrum, including the most popular algorithm due to Eckmann *et al.* [18], require a very long time series which is impractical. Further, all modified algorithms including those suited for short (such as the PLC *h* file) time series [26], also fail in the presence of noise level larger than 2% [27]. (The noise levels in our time series are not known.) For this reason, we have effected a modification of the Eckmann's algorithm which is suitable for *short time series* in the presence of *high levels of noise*. The method is outlined and illustrated elsewhere [28,29]. Here we briefly recall the central point. Eckmann's algorithm relies on connecting the initial small difference vectors $\vec{\xi}_i-\vec{\xi}_j$ to the evolved difference vectors through a set of tangent matrices. The vectors $\vec{\xi}_j$ used as neighbors of $\vec{\xi}_i$ on the reference trajectory are those contained within a shell size ϵ_s around $\vec{\xi}_i$. The number of neighbors used is usually taken to be $\min[2d,d+4]$. However, so few points cannot be expected to properly sample the statistics of uncorrelated noise which corrupts the original signal whose effect we wish to average out. Thus the basic idea is to *sample the statistics of noise properly by including enough neighbors within the shell size* ϵ_s subject to the following conditions. For a chaotic dynamics we should ensure that (a) the sum of the Lyapunov exponents is negative as required for a dissipative system, (b) there exists a stable zero exponent, and (c) *stable* values of the positive Lyapunov exponent emerge when we vary the shell size (and the time lag) in a certain range. (By ''stable,'' we mean constancy as a function of these parameters. Once this is done, we expect that both the positive and zero exponents of a deterministic chaotic signal remain *stable* over a fair interval of the shell size ϵ_s. Here we mention that this improved algorithm is capable of detecting the existence of positive and zero exponents for high levels of noise and short time series ($\sim$6000), as we have shown for the Lorenz system with noise levels up to 15% of the mean amplitude of the time series [28,29]. Apart from this, we have also shown that the Lyapunov spectrum for the surrogate data sets of chaotic time series do not exhibit a stable positive Lyapunov exponent or zero exponent as a function of the shell size ϵ_s. The method is also capable of estimating the superposed noise level. We shall use this method for the analysis of the time series.

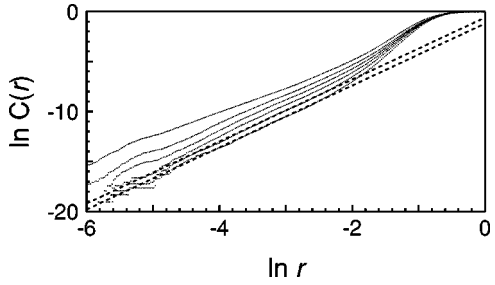

FIG. 2. Log-log plot of the correlation integral $C(r)$ vs r for the PLC m file for $d=4-9$. The dashed line is shown as a guide to the eye with an exponent value $\nu=2.7$.

Looked at from the point view of dynamics, a SOC signal is different from a chaotic one. There is a power law growth of any disturbance [30] as against an exponential growth in chaotic dynamics. Thus we expect that the improved algorithm shows no stable positive Lyapunov exponent for the time series which exhibits scaling distribution.

IV. RESULTS

A. Low and medium strain rates

Since the methods used and the results obtained are very similar for the low and medium PLC strain rate files l and m, we illustrate the results with that of the PLC file m mentioning the differences from the PLC file l when they exist. In both cases, the distribution of stress drops is peaked, with a single peak for the PLC l data and two peaks for the PLC m case. The autocorrelation function displays an oscillatory trend once it crosses the zero value with a large autocorrelation time $t_c \sim 35$. (We take t_c to be the time at which the autocorrelation function falls to $1/e$ of its original value.) Using a slightly smaller delay time $\tau=20$, we have calculated the correlation integral $C(r)$ shown in Fig. 2 from $d=4$ to 9. A scaling region of two orders of magnitude can be seen in the interval $-4.0<\ln r<-2.0$, with the slopes $\ln C(r)/\ln r$ converging as the embedding dimension approaches $d=9$. The resulting correlation dimension is about 2.7. As a guide to the eye, dashed lines show the converged slopes for $d=8$ and 9.

A similar exercise was carried out on all surrogate data sets keeping the same time delay τ. In Fig. 3 we have shown the slopes $\ln C(r)/\ln r$ in the same scaling regime as for the original file from $d=4$ (○). It is clear that the slopes keep

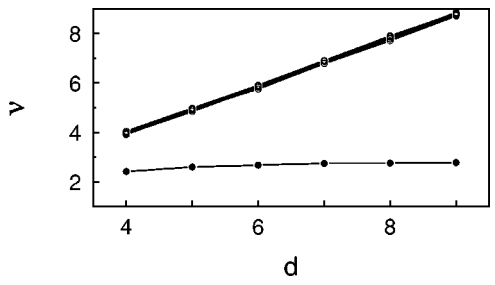

FIG. 3. Plot of the estimated scaling exponent ν of the correlation integral $C(r)$ in the scaling region as a function of d for several surrogate data sets (○ with lines) for the PLC m file. Also shown is the convergence of the exponent as a function of d for the original data (● connected by a line).

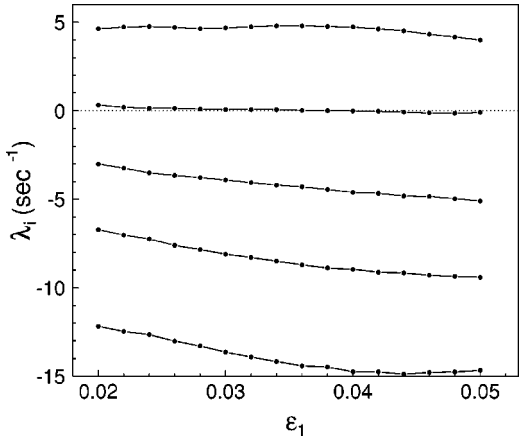

FIG. 4. Plot of the Lyapunov spectrum λ_i, $i=1-5$, as a function of the shell size ϵ_1 for the PLC m file (● connected by lines). The dotted line shows the zero value.

increasing with d, implying that there is no converged value for the slope. For the sake of comparison, the convergence of the slope in the scaling regime for the original signal is also shown (●).

Before proceeding with the calculation of the Lyapunov spectrum for the time series, we briefly outline the procedure followed. First the correlation time t_c is obtained from the time series. Using a time delay $\tau \sim t_c$, we calculate the Lyapunov spectrum for a judiciously chosen embedding dimension d for a range of values of the outer radius ϵ_1, keeping the inner radius ϵ_0 fixed. Usually, for $\tau \sim t_c$, the condition is violated for some values of ϵ_1. (The λ_i's here correspond to the converged values of λ_i as a function of time.) Therefore, τ is decreased until this condition is satisfied over the *entire range* of ϵ_1. For such a τ, λ_1 will be generally constant over a fair interval of ϵ_1, and does not change much as τ is reduced further. However, generally there will be no exponent whose value is close to zero. Therefore, τ is further decreased until we obtain an exponent λ_2 whose value is close to zero over a fair interval of ϵ_1 for which λ_1 is also constant.

Following this procedure, we have used $d=5$ and the inner shell radius $\epsilon_0=0.5\%$, and varied the outer radius ϵ_1. For a fixed time delay τ, the Lyapunov spectrum is calculated as a function of ϵ_1, and stable values of the positive and zero exponents λ_1 and λ_2 are looked for over a fair interval of ϵ_1, generally from 1% to 6%. Since t_c is large, the range over which τ must be scanned is wide. Starting from $\tau \sim 15$, as we decrease τ, we find that the sum of Lyapunov exponents is not negative until the value $\tau=10$ is reached. At this point, there is a stable value of the positive exponent λ_1, but there is no exponent whose value is close to zero. Since a zero exponent is one of the characteristic features of a deterministic system, the time delay τ is further decreased. We find that λ_2 is close to zero when $\tau=2$. For this delay, a stable positive exponent λ_1 is also obtained. The Lyapunov spectrum for $\tau=2$ is plotted in Fig. 4. (Each point in the plot corresponds to the converged value of λ_i as a function of time.) It is clear that both λ_1 and λ_2 are constant in the interval $2.0\%<\epsilon_1<4.5\%$. Actually, λ_2 is constant up to 6%, over a larger range than λ_1 (not shown in the figure).

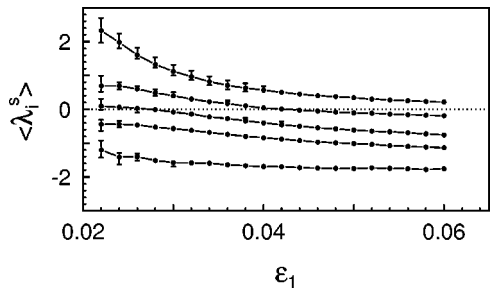

FIG. 5. Plot of the mean Lyapunov spectrum $\langle \lambda_i^s \rangle$, $i=1-5$, over 18 surrogate data sets as a function of the shell size ϵ_1 for the PLC *m* file (●). The dispersion is also shown. Note that there is no stable positive or zero exponent. The dotted line shows the zero value.

A similar analysis has been carried out on all surrogate data sets. Plots of the mean Lyapunov spectrum (over 18 samples) $\langle \lambda_i^s \rangle$, $i=1$ to d, along with the dispersions are shown in Fig. 5. As can be seen, both $\langle \lambda_1^s \rangle$ and $\langle \lambda_2^s \rangle$ show a decreasing trend in the entire range of ϵ_1. (All other $\langle \lambda_i \rangle$'s are also decreasing.) Further, the Lyapunov exponents of all the surrogate data sets behave in a similar manner which is reflected in the small dispersions, particularly in the range of ϵ_1 values for which λ_1 and λ_2 are stable for the original data. Further, we do not find any time delay τ such that $\langle \lambda_1^s \rangle$ and $\langle \lambda_2^s \rangle$ are stable.

Thus the evidence in support of chaos for the PLC *m* file is strong, as is clear from the existence of a finite correlation dimension, a stable positive Lyapunov exponent λ_1 and a stable zero exponent λ_2. Moreover, stable positive and zero exponents are absent for the corresponding surrogate data sets. On the basis of these results, we conclude that the time series is of chaotic origin. As already mentioned, very similar results are obtained for the low strain rate PLC *l* file with stable positive and zero Lyapunov exponents (over a similar range of ϵ_1) and the same value of the correlation dimension (with a slightly smaller scaling region). Again, the corresponding surrogate data sets for this file do not show finite correlation dimension and positive Lyapunov exponent.

B. High strain rate

.

Now, consider the analysis of the PLC *h* file corresponding to the highest strain rate. The distribution of stress drops in this case is no more peaked as the earlier two. Instead it shows a scaling form with an exponent α:

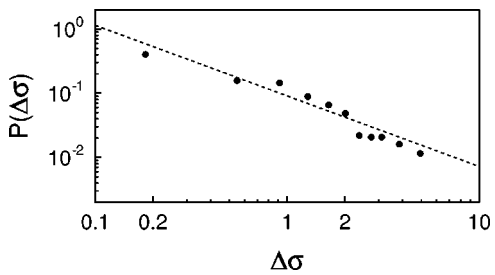

FIG. 6. Log-log plot of the distribution of the magnitude of the stress drops for the PLC *h* file (●). The dashed line shown is a fit obtained with $\alpha=1.1$.

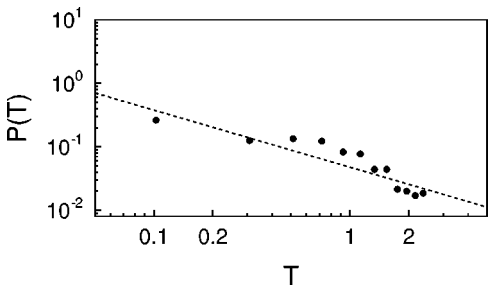

FIG. 7. Log-log plot of the distribution of the time intervals between stress drops for the PLC *h* file (●). The dashed line shown is a fit obtained with $\beta=0.9$.

$$P(\Delta\sigma)\sim\Delta\sigma^{-\alpha}. \tag{5}$$

A log-log plot of the normalized distribution $P(\Delta\sigma)$ is shown in Fig. 6. The dashed line corresponds to an exponent value $\alpha\sim1.1$. In Fig. 7 we also show the normalized distribution of the time duration of the stress drops T (which is a multiple of Δt) having a scaling form

$$P(T)\sim T^{-\beta}. \tag{6}$$

Clearly, there is a scatter in the midrange of T. Actually, it is known that, even in numerical simulations, the distribution of the duration of events is not as impressively scaled as that of the event sizes [17]. In the PLC effect, this is largely due to the shortness of the plastic relaxation time compared to the time interval at which σ is recorded ($\Delta t\sim0.05$ s). Even so, a rough estimate of the exponent β is still possible which we find to be $\beta\sim0.9$ (dashed line).

The magnitude of the events scales with their duration according to a power law given by

$$\Delta\sigma\sim T^{1/x}. \tag{7}$$

In practice, since time is monitored at finite intervals Δt, there is a distribution of stress drops for each value of T. Thus one can also plot the average magnitude of the stress drops as a function of their duration. Figure 8 displays a plot of $\langle \Delta\sigma \rangle$ versus T showing an exponent value $x=1.25$. The three exponents α, β, and x are related to each other through the scaling relation $\alpha=x(\beta-1)+1$. Clearly, this is satisfied quite well. However, since the confidence level in β is not high due to the scatter in Fig. 7, an independent check is needed which can be done by using the alternate scaling relation derived by Kertész and Kiss [31], connecting α and

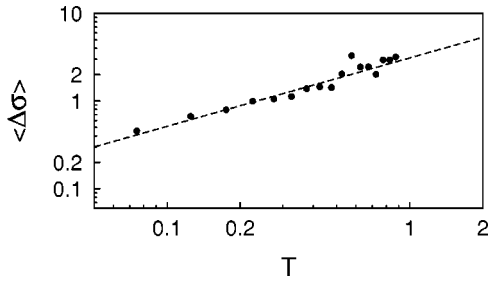

FIG. 8. Log-log plot of the mean of the stress drops as a function of the duration of the stress drops for the PLC *h* file (●). The dashed line shown is a fit obtained with $x=1.25$.

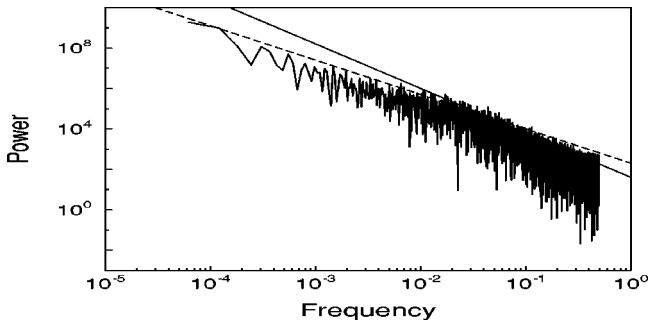

FIG. 9. Power spectrum corresponding to the PLC *h* file. The dashed line corresponds to a fit for the low-frequency region with an exponent 1.55. The solid line fits the high-frequency part, and has an exponent 2.05.

x to the low-frequency exponent of the Fourier power spectrum of the time series. Assuming that the total energy dissipation stems from independent elementary events whose energy density spectrum is quasi-Lorentzian, these authors have shown that if the scaling exponents satisfy the inequality

$$2x+\alpha>3, \tag{8}$$

the low-frequency power spectrum $S(\omega)$ behaves as

$$S(\omega)\sim\omega^{-(3-\alpha)/x}. \tag{9}$$

Using the values obtained for α and x, we see that inequality (8) holds, and we obtain $S(\omega)\sim\omega^{-1.48}$. The power spectrum of the time series is shown in Fig. 9. The low-frequency region has a scaling behavior shown by the dashed line with an exponent value 1.55, clearly consistent with the value 1.48 obtained from Eq. (9). (For higher frequencies, the power spectrum has a different scaling with an exponent value 2.05 shown by the continuous line.) This also implies that that the autocorrelation function also scales, i.e., $C(\tau)\sim\tau^{-\phi}$. We find a good scaling region with $\phi=0.37$.

The correlation dimension and Lyapunov spectrum are now calculated in order to understand these results from a dynamical point of view. For this file, t_c is much larger than the earlier two files. For a decay time $\tau=70$, the calculated correlation integral $C(r)$ is displayed in Fig. 10. As can be seen, there is no convergent scaling region as the embedding dimension is increased which is in sharp contrast to the results on two earlier data sets. [We have verified that the behavior of $C(r)$ is the same for all other τ values.]

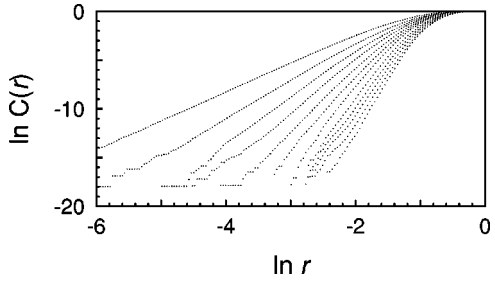

FIG. 10. Log-log plot of $C(r)$ vs r for the PLC *h* file for $d=3$–14. Note the lack of convergence of the slope.

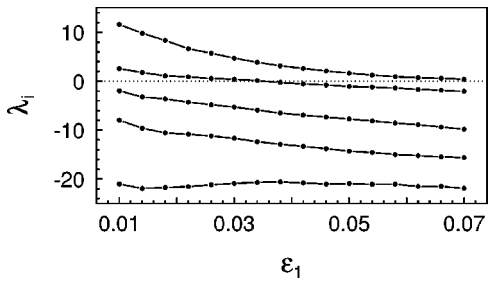

FIG. 11. Plot of the Lyapunov spectrum λ_i, $i=1$–5, as a function of the shell size ϵ_1 (● joined by lines) for the PLC *h* file. Note that there is no stable positive or zero exponent. The dotted line represents the zero value.

We proceed with the calculation of the Lyapunov spectrum for the PLC *h* file, keeping the inner shell radius $\epsilon_0=0.05\%$ for $d=5$. Since t_c is much larger than for the earlier two cases, the range over which τ need to be scanned is considerably larger. For a given choice of τ, the Lyapunov spectrum is computed as a function of the outer radius ϵ_1. Only below $\tau\sim15$, do we find that the sum of the Lyapunov exponents is negative in the entire range of ϵ_1. However, at this stage, we do not find a stable positive exponent λ_1, as a function of ϵ_1, as was the case for the two earlier files. *Moreover, as τ is further reduced, we are unable to obtain stable values of positive and zero exponents for any value of τ.* As an illustration, a plot of the Lyapunov spectrum for $\tau=1$ is shown in Fig. 11. Clearly, λ_1 has a decreasing tendency to zero, and λ_2 becomes negative as ϵ_1 is increased in the range $1.0\%<\epsilon_1<7\%$. This is in sharp contrast to the stable values of λ_1 and λ_2 obtained as a function of ϵ_1 for the PLC *l* and *m* data sets. This result should again be taken as indicative of the crossover in the nature of the underlying dynamics.

We have calculated both the correlation integral and Lyapunov spectrum for a number of surrogate data sets obtained from the PLC *h* file, keeping the same value of the time delay τ. The results on the correlation integral and Lyapunov spectrum were similar to the original file; no converged value of the slope $\ln C(r)/\ln r$ could be found, and no stable positive or zero Lyapunov exponent could be found. Thus the original signal and the surrogates are not distinguishable. This is in marked contrast to the PLC data sets *l* and *m*, where the original files and the surrogates behave very differently. Therefore, these results must be taken as an additional support for the crossover reflected in accompanying changes in the underlying dynamics as the strain rate is increased.

V. DISCUSSION AND CONCLUDING REMARKS

As the single crystal PLC time series *l*, *m*, and *h* offer a wide range of strain rate variations and reasonably long time series, they provide a suitable basis for the analysis of dynamical regimes of the PLC effect. Further, single crystals present the advantage of exhibiting crystallographic strain localization, parallel to the slip planes of the mobile dislocations, which can be thoroughly investigated by high speed cinematography and optical analysis of the slip steps left by dislocations emerging at free surfaces [32].

We have shown in this paper that the low and medium strain rate PLC files *l* and *m* are chaotic, characterized by stable positive and zero Lyapunov exponents and finite correlation dimensions; concomitantly their stress drop distributions are peaked. In contrast, the high strain rate PLC file *h* exhibits power law distributions for the magnitude and duration of the stress drops. The autocorrelation function and the power spectrum also exhibit power laws. These features are reminiscent of the SOC state [17], where events of all length scales and time scales occur, with power law distributions. In such a dynamics, any disturbance grows as a power law in time, implying the absence of a positive Lyapunov exponent [30]. Indeed, no stable positive Lyapunov exponent could be detected for the PLC *h* file. In addition, relations connecting the various scaling exponents have been found to be consistent with SOC-type dynamics. Further, a finite correlation dimension is absent for this case. *Thus, a crossover from chaos to a SOC-type dynamics has been identified as the applied strain rate is increased within the range of the PLC effect.* To the best of the authors' knowledge, this is the first experimental report in the literature of such a crossover. We stress that power law distributions have been observed for a range of values of high strain rates. Additional extensive experiments [33] also suggest that similar crossover might occur in Al-Mg polycrystals, and possibly in Al-Mg single crystals, where the statistics of stress drops also evolve from peaked to monotonously decreasing distributions.

This crossover has not been explained or modeled so far. However, it is likely that physical factors that may affect the observed dynamics are the instability mechanism itself, i.e., the existence of an anomalous force versus flux response of the dislocations, and the spatial coupling existing between the various defect populations.

The instability mechanism reviewed above in Sec. I can be better described as follows. When the applied strain rate is in the range where the PLC effect manifests itself, the local plastic strain rate is bivalued, with one low value corresponding to pinned dislocations, and the other, with a much higher value, to freed dislocations. (See Ref. [34] for more details. See also Ref. [6], where this negative strain sensitivity has been shown to result from nonlinear interaction of dislocations.) Starting from the pinned state at any location in the sample, the access to the unpinned state requires a finite fluctuation which is provided by a gradual loading of the sample. Then the local strain rate jumps to a higher level, eventually jumping back to the pinned state. The reloading time as well as the jump in the local strain rate depend on the applied overall strain rate. Both decrease due to the negative strain rate sensitivity as the applied strain rate increases.

Spatial coupling, whose origin is still a matter of debate, is responsible for the widening and propagation of bands of localized plastic deformation. In single crystals, it may stem either from dislocation mechanisms or from geometrical incompatibilities between slipped and unslipped regions. At present, it is believed that these incompatibilities are accommodated elastically but can be also partly relaxed by plastic flow, with a certain relaxation time. The magnitude of the coupling is at a maximum when elasticity alone is involved; it decreases with increasing plastic relaxation, the latter being favored by material or experimental conditions that lower the flow stress. Since the strain rate sensitivity of the flow stress is negative, the magnitude of spatial coupling decreases as the applied strain rate increases. Thus the plastic relaxation time increases with the applied strain rate.

The crossover might be expected as the plastic relaxation time becomes comparable with the characteristic reloading time. At low strain rates, the reloading time is larger than the plastic relaxation time. In such conditions, incompatibilities are fully relaxed within the reloading time and, in space, within a characteristic relaxation length scale which allows for stress drop uniformization. Within the spatial elements where the relaxation is complete, different types of dislocation populations themselves interact in nonlinear way leading to chaos [6]. At a sufficiently high applied strain rate, the plastic relaxation time becomes larger than the reloading time. Then new small inhomogeneities can form before plastic relaxation is complete. This picture results in a recurrence of partial relaxation processes, each time with a different magnitude, which in turn may provide stress drop distributions without a characteristic value. Partial relaxation of spatial nonuniformities entails ''diffusion'' of dislocation populations into the neighboring material elements, which may lead to a SOC-type dynamics. Following these ideas, additional experiments in single crystals, as well as further modeling, are required to understand more thoroughly the causes of the crossover.

ACKNOWLEDGMENTS

The data provided by Professor Neuhauser's group in Braunschweig Technical University is gratefully acknowledged. This work was supported by Indo-French Centre for the Promotion of Advanced Research (IFCPAR, New-Delhi, India) under Contract No. 1108-1, CNRS/PICS Program No. 657, and JNCASR. Support from these agencies is also gratefully acknowledged. One of the authors (G.A.) would like to acknowledge the support of the University of Metz for his stay at Metz during 1998 and 1999.

[1] A. H. Cottrell, *Dislocations and Plastic Flow in Crystals* (Clarendon Press, Oxford, 1953).
[2] J. Friedel, *Dislocations* (Pergamon Press, Oxford, 1964).
[3] L. P. Kubin and Y. Estrin, Scr. Metall. Mater. **29**, 1147 (1993).
[4] A. van den Beukel, Phys. Status Solidi A **30**, 197 (1975).
[5] P. Penning, Acta Metall. **20**, 35 (1972).
[6] G. Ananthakrishna and M. C. Valsakumar, J. Phys. D **15**, L171 (1982); the basic model was formulated in G. Ananthakrishna and D. Sahoo, J. Phys. D **15**, 2081 (1981).
[7] G. Ananthakrishna and M. C. Valsakumar, Phys. Lett. A **95**, 69 (1983).
[8] G. Ananthakrishna and T. M. John, in *Directions in Chaos*, edited by Hao Bai-Lin (World Scientific, Singapore, 1990), p. 133.
[9] V. Jeanclaude, C. Fressengeas, and L. P. Kubin, in *Nonlinear Phenomena in Materials Science II*, edited by L. P. Kubin and G. Martin (Trans Tech, Aldermanndorf, 1992), p. 385.
[10] G. Ananthakrishna, C. Fressengeas, M. Grosbras, J. Vergnol, C. Engelke, J. Plessing, H. Neuhauser, E. Bouchaud, J. Planès, and L. P. Kubin, Scr. Metall. Mater. **32**, 1731 (1995).

[11] P. Grassberger and I. Procaccia, Physica D **9**, 189 (1983).
[12] G. Ananthakrishna and S. J. Noronha, in *Non Linear Phenomena in Materials Science III*, edited by G. Ananthakrishna, L. P. Kubin, and G. Martin, Solid State Phenomena Vols. 42 and 43 (Scitec, Zug, Switzerland, 1995), pp. 277–286; S. J. Noronha, G. Ananthakrishna, L. Quaouire, and C. Fressengeas, Pramana, J. Phys. **48**, 705 (1997).
[13] S. J. Noronha, G. Ananthakrishna, L. Quaouire, C. Fressengeas, and L. P. Kubin, Int. J. Bifurcation Chaos Appl. Sci. Eng. **7**, 2577 (1997).
[14] S. Venkadesan, K. P. N. Murthy, S. Rajasekhar, and M. C. Valsakumar, Phys. Rev. E **54**, 611 (1996).
[15] M. Lebyodkin, Y. Bréchet, Y. Estrin, and L. P. Kubin, Phys. Rev. Lett. **74**, 4758 (1995).
[16] M. Lebyodkin, Y. Bréchet, Y. Estrin, and L. P. Kubin, Acta Metall. **44**, 4531 (1996).
[17] P. Bak, C. Tang, and K. Wiesenfeld, Phys. Rev. A **38**, 364 (1988); Phys. Rev. Lett. **59**, 381 (1987).
[18] J. P. Eckmann, S. O. Kamphorst, D. Ruelle, and S. Ciliberto, Phys. Rev. A **34**, 4971 (1986).
[19] M. Sano and Y. Sawada, Phys. Rev. Lett. **55**, 1082 (1985).
[20] A. Wolf, J. B. Swift, H. L. Swinney, and J. A. Vastano, Physica D **16**, 285 (1985).
[21] A. Norton and Ch. Schwink, Acta Metall. **45**, 2043 (1997).
[22] N. H. Packard, J. P. Crutchfield, J. D. Farmer, and R. S. Shaw, Phys. Rev. Lett. **45**, 712 (1980).
[23] A. R. Osborne and A. Provenzale, Physica D **35**, 357 (1989).
[24] J. Theiler, S. Eubank, A. Longtin, B. Galdrikian, and J. D. Farmer, Physica D **58**, 77 (1992).
[25] A. Provenzale, L. A. Smith, R. Vio, and G. Murante, Physica D **58**, 31 (1992).
[26] X. Zeng, R. Eykholt, and R. A. Pielke, Phys. Rev. Lett. **66**, 3229 (1991).
[27] T. Schreiber and H. Kanz, in *Predictability of Complex Dynamical Systems*, edited by Y. A. Krastov and J. B. Kadtke (Springer, New York, 1996).
[28] S. J. Noronha and G. Ananthakrishna (unpublished).
[29] S. J. Noronha, Ph.D thesis, Indian Institute of Science, Bangalore, 1998.
[30] K. Chen, P. Bak, and S. P. Obukhov, Phys. Rev. **43**, 625 (1991).
[31] J. Kertesz and L. B. Kiss, J. Phys. A **23**, L433 (1990).
[32] H. Neuhauser, in *Dislocations in Solids*, edited by F. R. N. Nabarro (North-Holland Amsterdam, 1983), Vol. 6, p. 319.
[33] L. P. Kubin, G. Ananthakrishna, Y. Bréchet, Y. Estrin, C. Fressengeas, and M. Lebyodkin, in *The Integraton of Material, Process and Product Design*, edited by N. Zabaras, R. Becker, S. Gosh, and L. Lalli (A. A. Balkema, Rotterdam, Netherlands, 1999), p. 85.
[34] Y. Estrin and L. P. Kubin, in *Continuum Models for Materials with Microstructure*, edited by H. B. Mulhaus (Wiley, New York, 1995), p. 395.